

Silencing of keratin 15 impairs viability and mobility while facilitating the doxorubicin chemosensitivity by inactivating the β -catenin pathway in liver cancer

JUNYING WANG and GUANGYU ZHU

Department of Interventional Radiology and Vascular Surgery, Zhongda Hospital,
Southeast University, Nanjing, Jiangsu 210009, P.R. China

Received March 14, 2023; Accepted July 11, 2023

DOI: 10.3892/ol.2023.14034

Abstract. Keratin 15 (KRT15) regulates the invasion as well as the stemness and is associated with tumor size and metastasis of several gastrointestinal cancers apart from liver cancer. The present study aimed to explore the effect of KRT15 knockdown on liver cancer malignant behaviors and its interaction with the β -catenin pathway. Small interfering (si)-KRT15 and si-negative control (NC) were transfected into liver cancer cell lines, followed by the addition or not of CHIR-99021 (a β -catenin agonist). Cell viability, invasion, apoptosis, and the half maximal inhibitory concentration (IC_{50}) value of doxorubicin (Dox) were then assessed. The present study illustrated that KRT15 gene and protein expression levels were upregulated in most liver cancer cell lines (Huh7, PLC, Hep3B and HepG2) compared to the normal liver cell line THLE-2. si-KRT15 reduced cell viability and invasive cell count while promoting the apoptosis rate in Huh7 and HepG2 cells. In addition, si-KRT15 also reduced the IC_{50} value of Dox. Furthermore, si-KRT15 inactivated the β -catenin pathway as reflected by β -catenin, cyclin D1 and c-Myc expression levels in Huh7 and HepG2 cells. Subsequently, CHIR-99021 treatment increased the cell viability and invasive cell count while reducing the apoptosis rate in Huh7 and HepG2 cells. Concurrently, the IC_{50} value of Dox was also increased. Notably, CHIR-99021 treatment attenuated the effect of si-KRT15 on mediating the aforementioned Huh7 and HepG2 cell malignant behaviors and Dox chemosensitivity. In conclusion, KRT15 knockdown suppressed viability and mobility but facilitated Dox chemosensitivity via inactivating the β -catenin pathway in liver cancer, suggesting its potential as a target for liver cancer treatment.

Introduction

Liver cancer, the major subtype of primary liver cancer, is the fourth leading cause of cancer-related mortality worldwide (1,2). Although the precise pathophysiological mechanism of liver cancer remains obscure, some factors (such as viral infection, metabolism dysregulation, alcohol consumption) have been identified to be associated with the risk of liver cancer, thus improving the prevention and screening of liver cancer (3-6). However, most patients with liver cancer are diagnosed at an intermediate or advanced stage which renders radical treatment unavailable, resulting in limited curative options and a poor survival (7). Therefore, it is essential to reveal novel and valid molecular mechanisms of liver cancer progression to identify new treatment targets.

Keratin 15 (KRT15) is a type I intermediate filament that was originally identified in the basal cells of the epidermis and stratified squamous epithelia (8). According to previous studies, the carcinogenic property of KRT15 in several cancers has been identified (9-11). For instance, a previous study showed that KRT15 facilitated colorectal cancer cell migration and invasion in a β -catenin-dependent manner (9). Another study revealed that KRT15-positive breast ductal progenitors have similar transcriptomic signatures with basal-like breast cancer (10). In addition, a previous animal study reported that KRT15-positive crypt cells may originate intestinal cancer formation and are resistant to radiation (11). Clinically, KRT15 demonstrated the ability to predict prognosis in several gastrointestinal carcinomas including esophageal, gastric and colorectal cancer (12-14). However, the mechanism involved with regard to the function of KRT15 in liver cancer remains poorly elucidated.

Therefore, the aim of the present study was to explore the effect of KRT15 knockdown on liver cancer viability, mobility and chemoresistance, as well as its interaction with the β -catenin pathway.

Materials and methods

Cell lines. The normal liver cell line THLE-2 (Cat. No. iCell-h38) cell lines were provided by the iCell Bioscience Inc. and liver cancer cell lines including Huh7 (Cat. No. CL-0120), PLC

Correspondence to: Dr Guangyu Zhu, Department of Interventional Radiology and Vascular Surgery, Zhongda Hospital, Southeast University, 87 Dingjiaqiao Road, Nanjing, Jiangsu 210009, P.R. China
E-mail: njzgy@sina.com

Key words: liver cancer, keratin 15, cell malignant behaviors, doxorubicin chemosensitivity, β -catenin pathway

(Cat. No. CL-0415), Hep3B (Cat. No. CL-0102), HepG2 (Cat. No. CL-0103), and Li-7 (Cat. No. CL-0139) were obtained from Procell Life Science & Technology Co., Ltd. Cells of THLE-2 were maintained in BEGM (Lonza Group, Ltd.), cells including PLC, Hep3B, HepG2 and Li-7 were maintained in RPMI-1640 medium (Procell Life Science & Technology Co., Ltd.) and Huh7 cells were maintained in DMEM (Procell Life Science & Technology Co., Ltd.). The medium was supplemented with 10% fetal bovine serum (FBS; Sigma-Aldrich; MilliporeSigma) and 1% penicillin/streptomycin (Procell Life Science & Technology Co., Ltd.). All cells were cultured in a humidity incubator with 5% CO₂ at 37°C. The expression level of KRT15 in these cells was assessed using reverse transcription-quantitative PCR (RT-qPCR) and western blot analyses.

KRT15 regulation. The KRT15 small interfering (si)RNA (si-KRT15, 5' AGGAGTACAAGATGCTGCTTGACAT 3') and negative control (si-NC, scramble siRNA, 5' AGGATA CGATACGGTTCGTAGACAT 3'), KRT15 overexpression plasmid (oe-KRT15, pcDNA3.1 vector containing the cDNA of KRT15, NM_002275.4) and negative control overexpression plasmid (oe-NC, empty pcDNA3.1 vector) were acquired from GenScript. Huh7 and HepG2 cells were plated and transfected with 50 pM si-NC or si-KRT15, 0.8 µg oe-NC or oe-KRT15 in the presence of Lipofectamine[®] 3000 (Sigma-Aldrich; MilliporeSigma) according to the manufacturer's protocol at 37°C for 6 h. Untransfected cells served as the control group. After 72 h of culture, cells were collected for RT-qPCR and western blotting. Subsequently, Cell Counting Kit-8 (CCK-8), Annexin V/Propidium iodide (AV/PI), and Transwell assays were performed to assess the effect of KRT15 on the viability, apoptosis and invasion of liver cancer cells. The doxorubicin (Dox) sensitivity assay was carried out using the CCK-8 method.

CHIR-99021 treatment. CHIR-99021, an agonist of the β-catenin pathway, was used to assess the regulation of the β-catenin pathway by KRT15 in liver cancer cells. Huh7 and HepG2 cells were transfected as aforementioned. The 5x10⁵ transfected cells were then cultured for 24 h with or without CHIR-99021 treatment (5 µM; MedChemExpress) at 37°C. In addition, cells without transfection and CHIR-99021 treatment served as the control group. The concentration of CHIR-99021 was determined according to a previous study (15) and a preliminary experiment performed in the present study. Western blotting, CCK-8, AV/PI, Transwell, and drug sensitivity assays were performed.

RT-qPCR. Briefly, total RNA of THLE-2 or liver cancer cells was extracted using Beyozol (Beyotime Institute of Biotechnology). The RT-qPCR assays were carried out using a One-Step SYBR Green RT-qPCR Kit (Wuhan Servicebio Technology Co., Ltd.) according to the manufacturer's protocol. KRT15 gene expression was assessed using the 2^{-ΔΔC_q} method (16). The thermal cycles for qPCR were as followings: 98°C for 2 min (min), 1 cycle; 98°C for 15 sec (sec), 61°C for 20 sec, 40 cycles. The sets of primers were as follows: KRT15 forward, 5'-AGGACTGACCTGGAGATGCAGA-3' and reverse, 5'-TGCGTCCATCTCCACATTGACC-3'; GAPDH

forward, 5'-GAGTCCACTGGCGTCTTCAC-3' and reverse, 5'-ATCTTGAGGCTGTTGTCATACTTCT-3'.

Western blotting. Briefly, THLE-2 or liver cancer cells were lysed with RIPA buffer (Wuhan Servicebio Technology Co., Ltd.) and the concentration of total protein was measured using a BCA Protein Assay kit (Cat. No. ml095490; Shanghai Enzyme-Linked Biotechnology Co., Ltd.). The 20 µg protein was then separated by 4-20% SDS-PAGE and transferred to a nitrocellulose membrane (Beyotime Institute of Biotechnology). After being blocked with 5% BSA (Wuhan Servicebio Technology Co., Ltd.) for 90 min at 37°C, the membranes were incubated with primary antibodies at the recommended dilution ratio, including KRT15 (1:10,000; Cat. No. ab52816; Abcam), β-catenin (1:10,000; Cat. No. ab32572; Abcam), cyclin D1 (1:2,000; Cat. No. ab239794; Abcam), c-Myc (1:1,000; Cat. No. ab32072; Abcam), and GAPDH (1:10,000; Cat. No. ab8245; Abcam) at 4°C overnight. Subsequently, the membranes were incubated using diluted HRP linked secondary antibody (1:20,000; Cat. No. ab6721; Abcam) at 37°C for 1.5 h and detected using an ECL kit (Wuhan Servicebio Technology Co., Ltd.). The grey value was analyzed by Image J (1.0, NIH).

Cell viability assay. Briefly, the 3x10³ treated Huh7 and HepG2 cells were plated and cultured for 24 h at 37°C. The CCK-8 mixture (10 µl/well; APeXBio Technology LLC) was then used, and the cells were incubated for 2 h at 37°C. The optical density (OD) values were read using a microplate reader (Rayto Life and Analytical Sciences Co., Ltd.). The viability of Huh7 and HepG2 cells was evaluated according to the OD values.

Cell apoptosis assay. The apoptosis of treated cells was evaluated using an Annexin V-FITC/PI Kit (Nanjing Jiancheng Bioengineering Institute). Huh7 and HepG2 cells were collected, washed, and resuspended in Annexin V binding reagent. Subsequently, an Annexin V-FITC and PI mixture was added to the cells and incubated for 20 min at 37°C. Finally, the cells were analyzed using BD FACSCanto (BD Biosciences) and Flowjo 10 (BD Biosciences).

Transwell assay. Following treatment, the 4x10⁴ Huh7 and HepG2 cells were resuspended in FBS-free medium (DMEM for Huh7 cells, RPMI-1640 for HepG2) and seeded into the upper chamber of a Matrigel-coated Transwell plate (37°C for 1 h; Corning, Inc.). Complete medium (10% FBS-containing DMEM or RPMI-1640) was added to the lower chambers. After being cultured for 24 h at 37°C, the invasive cells were stained using crystal violet (Wuhan Servicebio Technology Co., Ltd.) for 20 min at room temperature and counted under an inverted light microscope (Leica Microsystems, Inc.; magnification was X200).

Drug sensitivity assay. A total of 5x10⁴ treated Huh7 and HepG2 cells were plated and stimulated with 0, 1, 2, 4, 8, 16, and 32 µM Dox (MedChemExpress) according to a previous study (17) and a preliminary experiment performed in the present study. After 48 h of incubation at 37°C, a CCK-8 assay was carried out as aforementioned, and the half maximal

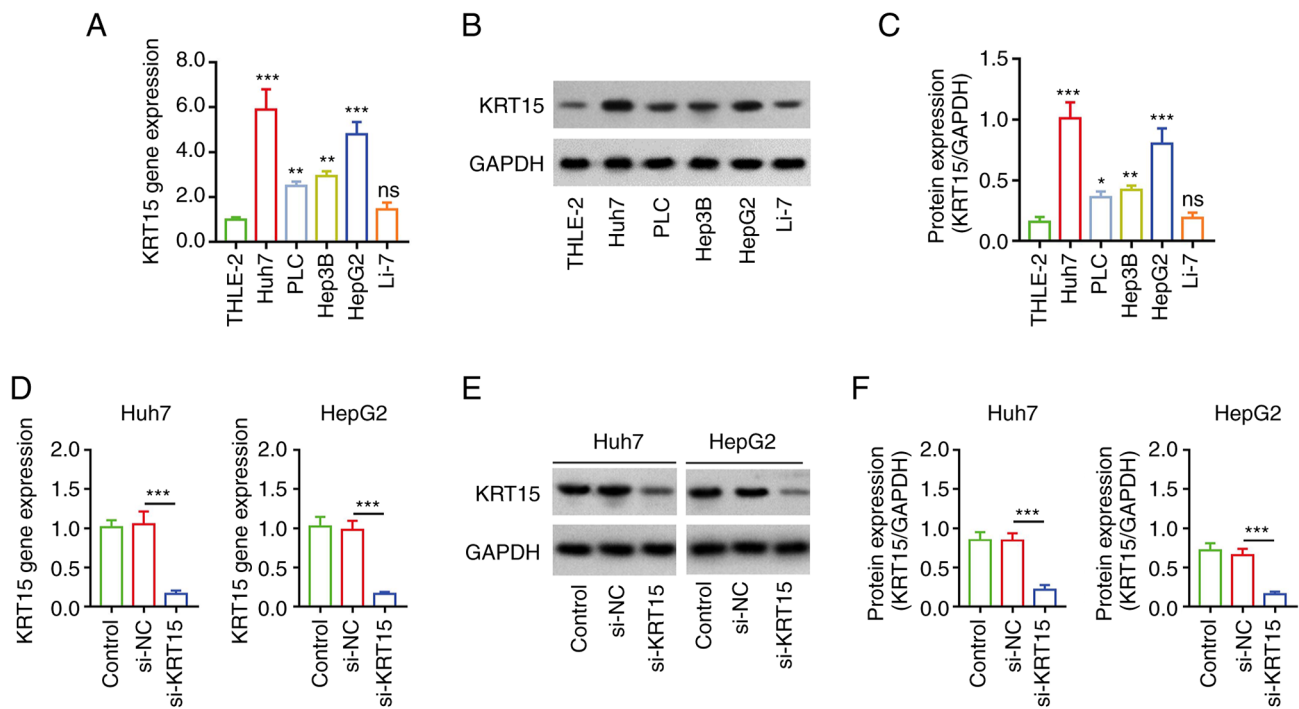


Figure 1. KRT15 expression is upregulated in liver cancer cell lines. (A) Comparison of KRT15 gene expression between liver cancer cell lines and a normal liver cell line. (B) Western blot analysis bands and (C) quantitative comparison of KRT15 protein expression between liver cancer cell lines and a normal liver cell line. (D) Comparison of KRT15 gene expression between si-NC and si-KRT15 groups in liver cancer cell lines, Huh7 and HepG2. (E) Western blot analysis bands and (F) quantitative comparison of KRT15 protein expression between si-NC and si-KRT15 groups in liver cancer cell lines, Huh7 and HepG2. * $P < 0.05$, ** $P < 0.01$ and *** $P < 0.001$. KRT15, keratin 15; si-, small interfering RNA; NC, negative control; ns, not significant.

inhibitory concentration (IC_{50}) of Dox was analyzed by a sigmoidal dose-response function curve (18).

Statistical analysis. The data (in triplets) were represented as mean \pm standard deviation. The comparisons were performed using one-way ANOVA with Tukey's or Dunnett's post hoc test. All analyses were performed using GraphPad Prism (V.7.0; GraphPad Software, Inc.; Dotmatics). $P < 0.05$ was considered to indicate a statistically significant difference.

Results

KRT15 expression among different cell lines. KRT15 gene expression was enhanced in liver cancer cell lines (including Huh7, PLC, Hep3B and HepG2 cells) compared with normal liver cell line, THLE-2 cells (all $P < 0.01$; Fig. 1A). Moreover, KRT15 protein expression was also increased in Huh7, PLC, Hep3B, and HepG2 cells compared with THLE-2 cells (all $P < 0.05$; Fig. 1B and C). Subsequently, Huh7 cells and HepG2 cells were selected for the following functional experiments, since they had the highest and second highest expression level of KRT15 among the cell lines. si-KRT15 was then transfected into Huh7 cells and HepG2 cells, leading to a decrease in KRT15 gene expression (both $P < 0.001$; Fig. 1D) as well as protein expression (both $P < 0.001$; Fig. 1E and F).

Effect of si-KRT15 on viability, apoptosis, invasion, and chemosensitivity in liver cancer cell lines. Following transfection, si-KRT15 reduced the viability of Huh7 cells ($P < 0.01$) and HepG2 cells ($P < 0.05$) compared with si-NC (Fig. 2A). Moreover, si-KRT15 enhanced the cell apoptosis rate in Huh7

cells ($P < 0.001$) and HepG2 cells ($P < 0.01$; Fig. 2B and C). In addition, si-KRT15 also reduced the invasive cell count in Huh7 cells ($P < 0.01$) and HepG2 cells ($P < 0.05$; Fig. 2D and E). Subsequently, the effect of si-KRT15 on chemosensitivity to Dox in liver cancer cell lines was explored. It was observed that si-KRT15 reduced the IC_{50} value of Dox in Huh7 cells ($P < 0.01$) as well as in HepG2 cells ($P < 0.05$) compared with si-NC (Fig. 3A and B), suggesting the enhancement of chemosensitivity to Dox.

Regulatory function of si-KRT15 on the β -catenin pathway. Subsequently, western blot analysis was performed to determine the effect of si-KRT15 on the β -catenin pathway. Notably, it was observed that si-KRT15 downregulated the expression of β -catenin ($P < 0.01$), cyclin D1 ($P < 0.01$), and c-Myc ($P < 0.05$) compared with si-NC in Huh7 cells (Fig. 4A and B). si-KRT15 also decreased the expression of β -catenin ($P < 0.05$) and cyclin D1 ($P < 0.05$), while it did not significantly affect the expression of c-Myc in HepG2 cells.

Effect of CHIR-99021 on si-KRT15-induced β -catenin inactivation. CHIR-99021 (an agonist of β -catenin) was added for subsequent experiments. CHIR-99021 upregulated the expression levels of β -catenin, cyclin D1, and c-Myc (all $P < 0.05$) compared with si-NC in liver cancer cell lines (Fig. 5A and B). Notably, CHIR-99021 attenuated the effect of si-KRT15 on regulating the β -catenin pathway. Furthermore, it was also observed that oe-KRT15 upregulated the expression levels of β -catenin, cyclin D1, and c-Myc, but si-KRT15 downregulated them, in the liver cancer cell lines (Fig. S1A and B).

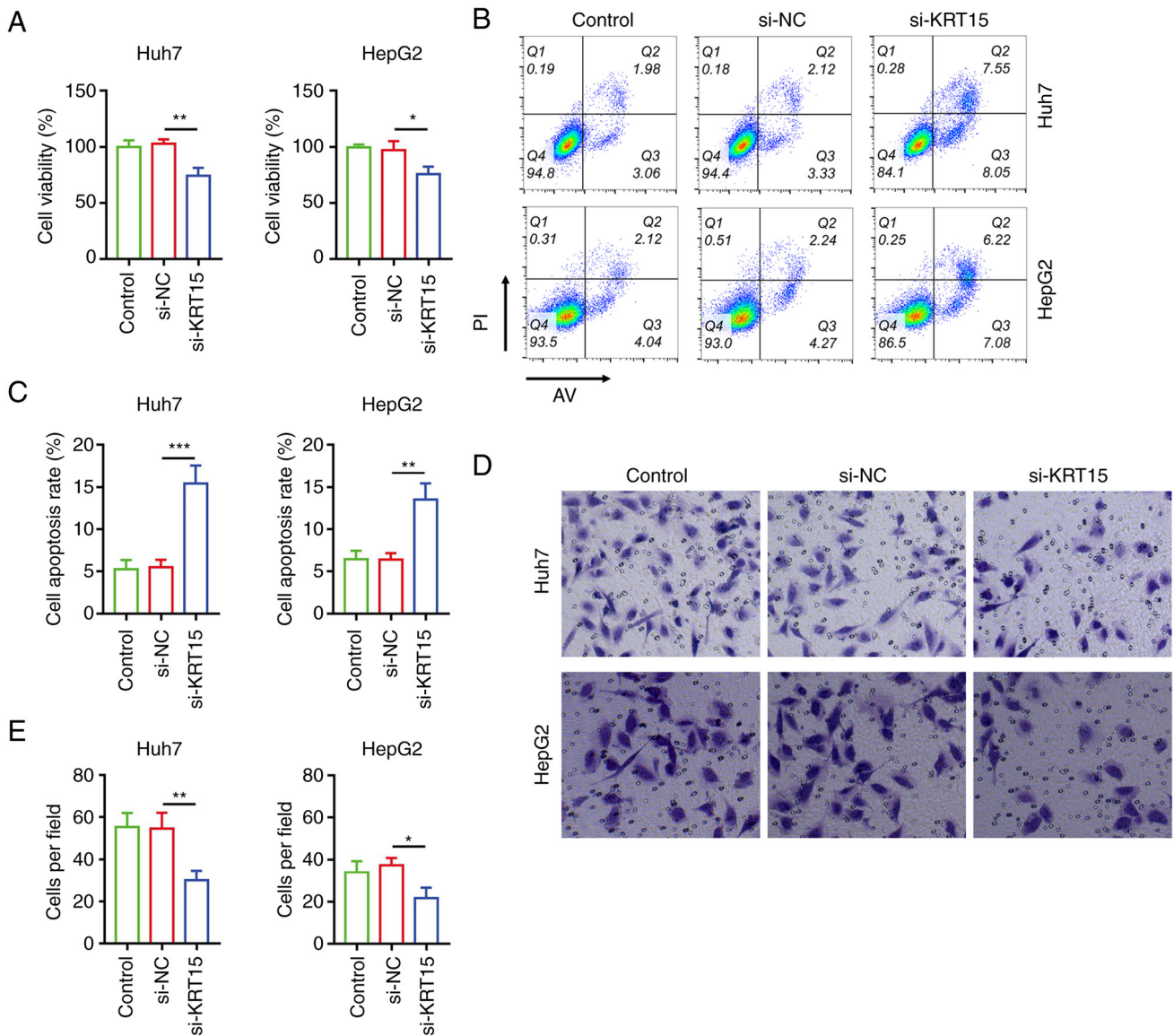


Figure 2. si-KRT15 reduces the viability and invasion of liver cancer cell lines. (A) Comparison of cell viability between si-NC and si-KRT15 groups in liver cancer cell lines. (B) Images of flow cytometric analysis and (C) quantitative comparison of cell apoptosis rate between si-NC and si-KRT15 groups in liver cancer cell lines. (D) Images of Transwell cell invasion (200 X) and (E) quantitative comparison of invasive cells between si-NC and si-KRT15 groups in liver cancer cell lines. * $P < 0.05$, ** $P < 0.01$ and *** $P < 0.001$. KRT15, keratin 15; si-, small interfering RNA; NC, negative control.

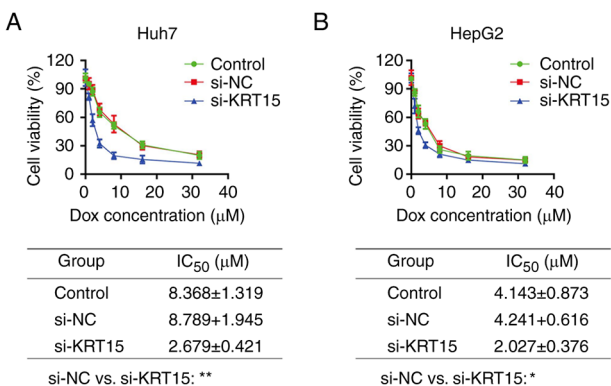


Figure 3. si-KRT15 enhances chemosensitivity to Dox. (A and B) Comparison of the IC₅₀ values of Dox between si-NC and si-KRT15 groups in (A) Huh7 cells and in (B) HepG2 cells. * $P < 0.05$ and ** $P < 0.01$. si-, small interfering RNA; KRT15, keratin 15; Dox, doxorubicin; IC₅₀, half maximal inhibitory concentration; NC, negative control.

Effect of CHIR-99021 on si-KRT15-modified liver cancer cell functions. CHIR-99021 treatment increased the viability of Huh7 cells ($P < 0.01$) and HepG2 cells ($P < 0.05$; Fig. 6A) compared with si-NC. However, CHIR-99021 treatment decreased the cell apoptosis rate in Huh7 cells ($P < 0.01$) and HepG2 cells ($P < 0.05$; Fig. 6B and C). Moreover, CHIR-99021 treatment enhanced the invasive cell count in Huh7 cells and HepG2 cells (both $P < 0.01$; Fig. 6D and E). Notably, CHIR-99021 treatment attenuated the effect of si-KRT15 on mediating cell viability, the apoptosis rate, and invasion in Huh7 cells and HepG2 cells (all $P < 0.01$; Fig. 6A-E).

Subsequently, it was also demonstrated that CHIR-99021 treatment greatly increased the IC₅₀ value of Dox in Huh7 cells ($P < 0.001$) and HepG2 cells ($P < 0.01$; Fig. 7A and B). In addition, CHIR-99021 alleviated the effect of si-KRT15 on regulating chemosensitivity to Dox in liver cancer cell lines (both $P < 0.01$).

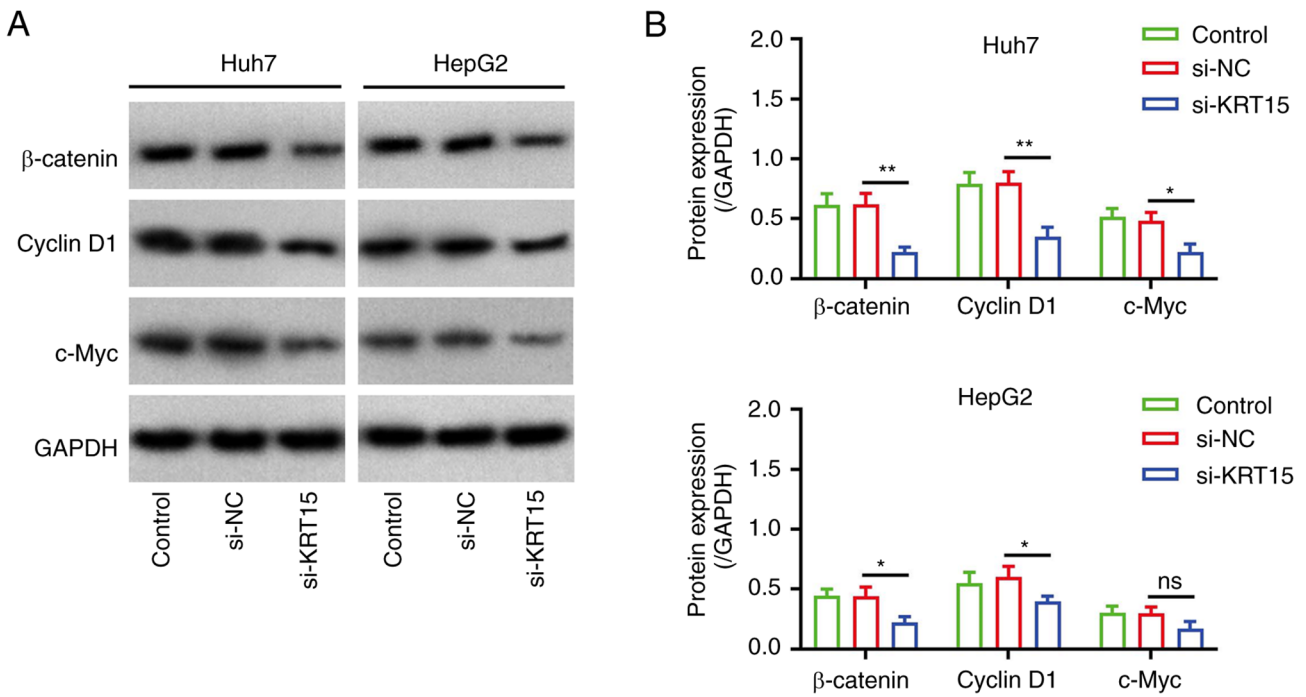


Figure 4. si-KRT15 inactivates the β -catenin pathway. (A) Western blot analysis bands and (B) quantitative comparison of β -catenin, cyclin D1, and c-Myc protein expression between si-NC and si-KRT15 groups in liver cancer cell lines. * $P < 0.05$ and ** $P < 0.01$. si-, small interfering RNA; KRT15, keratin 15; si-, small interfering RNA; NC, negative control; ns, not significant.

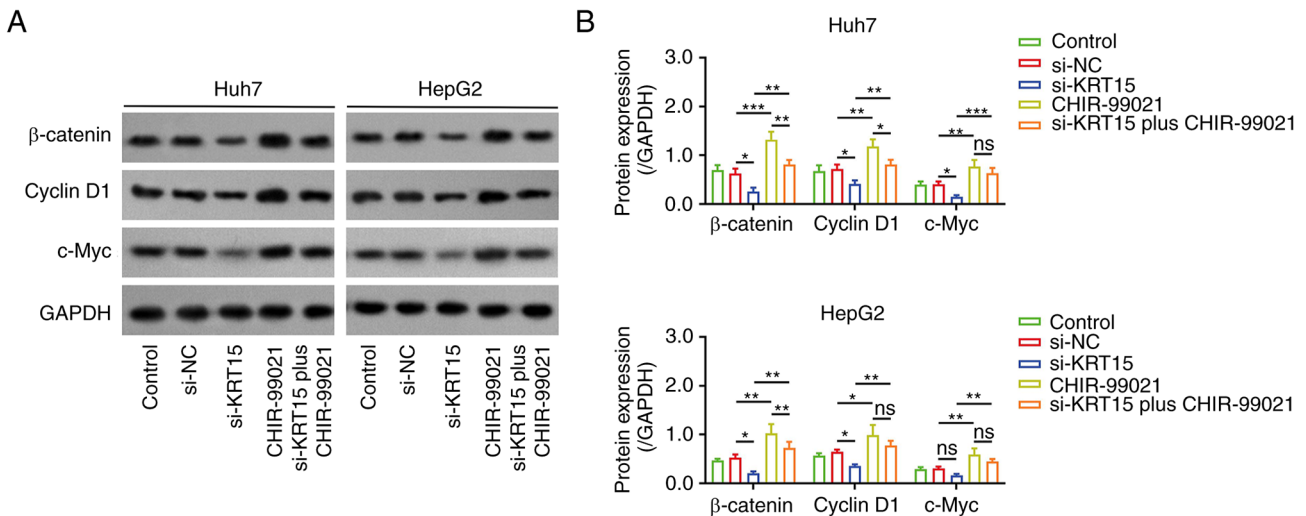


Figure 5. CHIR-99021 attenuates the effect of si-KRT15 on regulating the β -catenin pathway. (A) Western blot analysis bands and (B) quantitative comparison of β -catenin, cyclin D1, and c-Myc protein expression among si-NC, si-KRT15, CHIR-99021 and si-KRT15 plus CHIR-99021 groups in liver cancer cell lines. * $P < 0.05$, ** $P < 0.01$ and *** $P < 0.001$. si-, small interfering RNA; KRT15, keratin 15; NC, negative control; ns, not significant.

Discussion

In the clinical field, KRT15 exhibits diagnostic value and prognostic value in gastric, colorectal, endometrial, and breast invasive cancer (13,14,19,20). Regarding its application in patients with liver cancer, one previous bioinformatic study reported that KRT15 is an upregulated gene in patients with liver cancer with viral infection compared with controls (19). The present study detected KRT15 mRNA and protein expression in liver cancer cell lines and a normal liver cell line, and then observed an upregulation of KRT15 expression at both

the mRNA and protein levels in liver cancer cell lines. The possible explanation was that KRT15 reflected cell malignant growth and stemness, which were obviously elevated in the liver cancer cell lines versus the normal cell line; therefore, KRT15 demonstrated a higher trend in the liver cancer cell lines.

In addition, KRT15 was demonstrated to promote colorectal cancer cell mobility (9), and to be associated with tumor size, invasive degree, lymph-node metastasis, and increased TNM stage in patients with esophageal carcinoma and colorectal cancer (12,14). These previous studies indicate its implication

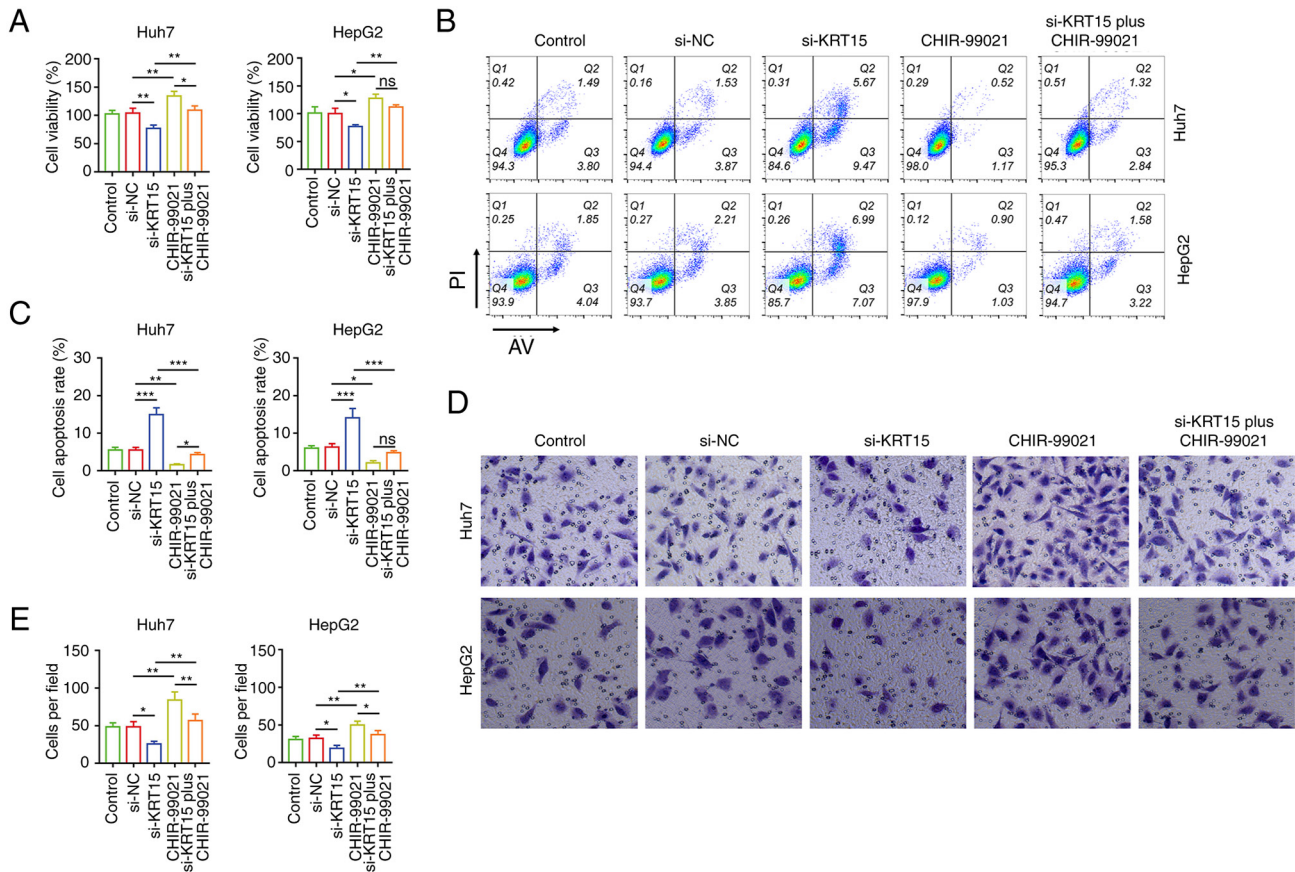


Figure 6. CHIR-99021 attenuates si-KRT15-induced viability and invasion of liver cancer cell lines. (A) Comparison of cell viability among si-NC, si-KRT15, CHIR-99021, and si-KRT15 plus CHIR-99021 groups in liver cancer cell lines. (B) Flow cytometric analysis and (C) quantitative comparison of the cell apoptosis rate among si-NC, si-KRT15, CHIR-99021, and si-KRT15 plus CHIR-99021 groups in liver cancer cell lines. (D) Images of Transwell cell invasion (200 X) and (E) quantitative comparison of invasive cells among si-NC, si-KRT15, CHIR-99021, and si-KRT15 plus CHIR-99021 groups in liver cancer cell lines. * $P < 0.05$, ** $P < 0.01$ and *** $P < 0.001$. si-, small interfering RNA; KRT15, keratin 15; NC, negative control; ns, not significant.

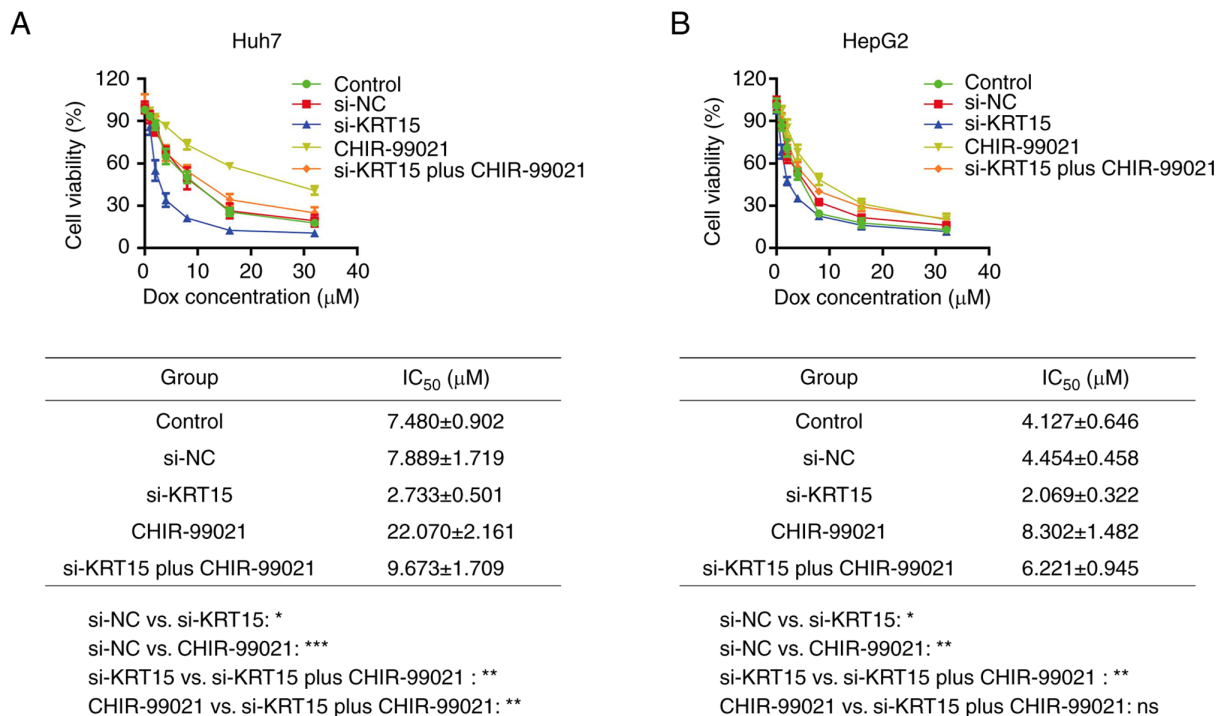


Figure 7. CHIR-99021 attenuates the effect of si-KRT15 on chemosensitivity to Dox in liver cancer cell lines. (A and B) Comparison of the IC₅₀ values of Dox among si-NC, si-KRT15, CHIR-99021 and si-KRT15 plus CHIR-99021 groups in (A) Huh7 cells and (B) HepG2 cells. * $P < 0.05$, ** $P < 0.01$ and *** $P < 0.001$. si-, small interfering RNA; KRT15, keratin 15; Dox, doxorubicin; IC₅₀, half maximal inhibitory concentration; NC, negative control; ns, not significant.

in regulating gastrointestinal carcinoma malignant behaviors. Furthermore, loss-of-function experiments revealed that KRT15 knockdown impaired viability and invasion, while it promoted the apoptosis rate in liver cancer cell lines, which could be explained as follows: i) KRT15 was associated with cancer stemness, the latter closely involved in the invasion of cancer cells (21,22), therefore, KRT15 knockdown reduced liver cancer cell invasion; and ii) KRT15 knockdown inactivated the β -catenin pathway (9), to repress the cell viability of liver cancer. These findings suggested that KRT15 serves as an oncogene in liver cancer pathogenesis, and its silencing could be a therapeutic option for liver cancer management.

Dox is a common type of anthracycline that exerts an antitumor effect in a wide spectrum of solid tumors (23). Regarding the application of Dox in treating patients with liver cancer, it is usually loaded during the transarterial chemoembolization (TACE) procedure which is a cornerstone for intermediate-stage liver cancer treatment (24,25). However, resistance to Dox may occur after several TACE procedures in patients with liver cancer, which further impairs their response and survival (26,27). Some aspects have been revealed to be involved in the chemoresistance of liver cancer, such as stemness, DNA damage repair, ATP binding cassette, etc. (28,29). In addition, identifying molecules that are involved in acquiring chemoresistance to Dox may serve as one crucial method to enhance chemosensitivity and therapeutic outcomes for liver cancer management. In the present study, the viability of liver cancer cell lines transfected with si-KRT15 under different Dox concentrations was determined, and then IC_{50} values of doxorubicin were also calculated. It was then revealed that KRT15 knockdown enhanced the chemosensitivity to Dox in liver cancer cell lines, indicating the potential therapeutic value of KRT15 knockdown for enhancing the response to Dox. The possible explanation was that KRT15 knockdown weakened the cancer stemness, thus restoring the sensitivity of chemotherapeutics (21,22,30). However, Dox-resistant liver cancer cell lines were not established in the present study, which served as a limitation for comprehensively analyzing the effect of KRT15 on chemoresistance. Besides, The lack of *in vivo* validation is also another limitation of the study.

The β -catenin pathway is a well-established oncogenic pathway in liver cancer (31). The canonical β -catenin pathway involves binding of Wnt to its membrane receptors followed by the upregulation of β -catenin, which further forms the destruction complex and translocates to the nucleus to initiate the expression of cell division-related transcription factors (such as c-Myc and cyclin D1) for carcinogenesis (31-33). In a previous study, KRT15 was shown to promote the β -catenin-mediated MMP7 pathway in colorectal cancer (9). In line with this previous study, KRT15 knockdown inactivated the β -catenin pathway in liver cancer in the present study. In addition, CHIR-99021, an agonist for β -catenin that activates the β -catenin pathway in endodermal differentiation, follicle development, and cerebral organoids (34-36), was added for subsequent compensative experiments in the present study. It was discovered that CHIR-99021 enhanced viability and invasion while reducing chemosensitivity to Dox in liver cancer cell lines, which could be due to activation of the β -catenin pathway (37,38). Furthermore, the present study also observed

that the administration of CHIR-99021 alleviated the effect of KRT15 knockdown on cell viability, apoptosis, invasion and Dox chemosensitivity in liver cancer cell lines, which further confirmed the implication of the β -catenin pathway in the effect of KRT15 on liver cancer malignant behaviors. However, other types of β -catenin agonists could be applied in future studies to further validate the effect of β -catenin in KRT15-mediated liver cancer pathogenesis, and si-NC plus CHIR-99021 could be added to further confirm the effect.

In conclusion, KRT15 knockdown impairs viability and mobility while it enhances chemosensitivity to Dox by inactivating the β -catenin pathway in liver cancer, implying its potency as a treatment target of liver cancer. However, further validation is warranted.

Acknowledgements

Not applicable.

Funding

No funding was received.

Availability of data and materials

The datasets used and/or analyzed during the current study are available from the corresponding author on reasonable request.

Authors' contributions

JW and GZ contributed to study conception and design. Material preparation, data collection and analysis were performed by JW and GZ. JW wrote the first draft of the manuscript. JW and GZ confirm the authenticity of all the raw data. Both authors read and approved the final version of the manuscript.

Ethics approval and consent to participate

Not applicable.

Patient consent for publication

Not applicable.

Competing interests

The authors declare that they have no competing interests.

References

1. Vogel A, Meyer T, Sapichochin G, Salem R and Saborowski A: Hepatocellular carcinoma. *Lancet* 400: 1345-1362, 2022.
2. Sung H, Ferlay J, Siegel RL, Laversanne M, Soerjomataram I, Jemal A and Bray F: Global cancer statistics 2020: GLOBOCAN estimates of incidence and mortality worldwide for 36 cancers in 185 countries. *CA Cancer J Clin* 71: 209-249, 2021.
3. Chidambaranathan-Reghupaty S, Fisher PB and Sarkar D: Hepatocellular carcinoma (HCC): Epidemiology, etiology and molecular classification. *Adv Cancer Res* 149: 1-61, 2021.
4. D'Souza S, Lau KC, Coffin CS and Patel TR: Molecular mechanisms of viral hepatitis induced hepatocellular carcinoma. *World J Gastroenterol* 26: 5759-5783, 2020.

5. Yang C, Huang X, Liu Z, Qin W and Wang C: Metabolism-associated molecular classification of hepatocellular carcinoma. *Mol Oncol* 14: 896-913, 2020.
6. Sasaki-Tanaka R, Ray R, Moriyama M, Ray RB and Kanda T: Molecular changes in relation to alcohol consumption and hepatocellular carcinoma. *Int J Mol Sci* 23: 9679, 2022.
7. Torimura T and Iwamoto H: Treatment and the prognosis of hepatocellular carcinoma in Asia. *Liver Int* 42: 2042-2054, 2022.
8. Moll R, Divo M and Langbein L: The human keratins: Biology and pathology. *Histochem Cell Biol* 129: 705-733, 2008.
9. Chen W and Miao C: KRT15 promotes colorectal cancer cell migration and invasion through β -catenin/MMP-7 signaling pathway. *Med Oncol* 39: 68, 2022.
10. Kohler KT, Goldhammer N, Demharther S, Pfisterer U, Khodosevich K, Rønnov-Jessen L, Petersen OW, Villadsen R and Kim J: Ductal keratin 15⁺ luminal progenitors in normal breast exhibit a basal-like breast cancer transcriptomic signature. *NPJ Breast Cancer* 8: 81, 2022.
11. Giroux V, Stephan J, Chatterji P, Rhoades B, Wileyto EP, Klein-Szanto AJ, Lengner CJ, Hamilton KE and Rustgi AK: Mouse intestinal Krt15⁺ crypt cells are radio-resistant and tumor initiating. *Stem Cell Reports* 10: 1947-1958, 2018.
12. Lin JB, Feng Z, Qiu ML, Luo RG, Li X and Liu B: KRT 15 as a prognostic biomarker is highly expressed in esophageal carcinoma. *Future Oncol* 16: 1903-1909, 2020.
13. Zhang C, Liang Y, Ma MH, Wu KZ and Dai DQ: KRT15, INHBA, MATN3, and AGT are aberrantly methylated and differentially expressed in gastric cancer and associated with prognosis. *Pathol Res Pract* 215: 893-899, 2019.
14. Rao X, Wang J, Song HM, Deng B and Li JG: KRT15 overexpression predicts poor prognosis in colorectal cancer. *Neoplasma* 67: 410-414, 2020.
15. Li Y, Liu Y, Liu B, Wang J, Wei S, Qi Z, Wang S, Fu W and Chen YG: A growth factor-free culture system underscores the coordination between Wnt and BMP signaling in Lgr5⁺ intestinal stem cell maintenance. *Cell Discov* 4: 49, 2018.
16. Livak KJ and Schmittgen TD: Analysis of relative gene expression data using real-time quantitative PCR and the 2(-Delta Delta C(T)) method. *Methods* 25: 402-408, 2001.
17. Lei KF, Liu TK and Tsang NM: Towards a high throughput impedimetric screening of chemosensitivity of cancer cells suspended in hydrogel and cultured in a paper substrate. *Biosens Bioelectron* 100: 355-360, 2018.
18. Tian S, Lou L, Tian M, Lu G, Tian J and Chen X: MAPK4 deletion enhances radiation effects and triggers synergistic lethality with simultaneous PARP1 inhibition in cervical cancer. *J Exp Clin Cancer Res* 39: 143, 2020.
19. Yang H, Li A, Li A, Zhao F and Zhang T: Upregulated keratin 15 links to the occurrence of lymphovascular invasion, stromal cervical invasion as well as unfavorable survival profile in endometrial cancer patients. *Medicine (Baltimore)* 101: e29686, 2022.
20. Zhong P, Shu R, Wu H, Liu Z, Shen X and Hu Y: Low KRT15 expression is associated with poor prognosis in patients with breast invasive carcinoma. *Exp Ther Med* 21: 305, 2021.
21. Zekri AN, El-Sisi ER, Abdallah ZF, Ismail A and Barakat Barakat A: Gene expression profiling of circulating CD133⁺ cells of hepatocellular carcinoma patients associated with HCV infection. *J Egypt Natl Canc Inst* 29: 19-24, 2017.
22. Abbas O, Richards JE, Yaar R and Mahalingam M: Stem cell markers (cytokeratin 15, cytokeratin 19 and p63) in in situ and invasive cutaneous epithelial lesions. *Mod Pathol* 24: 90-97, 2011.
23. Alam Khan S and Jawaid Akhtar M: Structural modification and strategies for the enhanced doxorubicin drug delivery. *Bioorg Chem* 120: 105599, 2022.
24. Chang Y, Jeong SW, Young Jang J and Jae Kim Y: Recent updates of transarterial chemoembolization in hepatocellular carcinoma. *Int J Mol Sci* 21: 8165, 2020.
25. Manjunatha N, Ganduri V, Rajasekaran K, Duraiyarsan S and Adefuye M: Transarterial chemoembolization and unresectable hepatocellular carcinoma: A narrative review. *Cureus* 14: e28439, 2022.
26. Al-Malky HS, Al Harthi SE and Osman AM: Major obstacles to doxorubicin therapy: Cardiotoxicity and drug resistance. *J Oncol Pharm Pract* 26: 434-444, 2020.
27. Buschauer S, Koch A, Wiggermann P, Müller M and Hellerbrand C: Hepatocellular carcinoma cells surviving doxorubicin treatment exhibit increased migratory potential and resistance to doxorubicin re-treatment *in vitro*. *Oncol Lett* 15: 4635-4640, 2018.
28. Marin JGG, Macias RIR, Monte MJ, Romero MR, Asensio M, Sanchez-Martin A, Cives-Losada C, Temprano AG, Espinosa-Escudero R, Reviejo M, *et al*: Molecular bases of drug resistance in hepatocellular carcinoma. *Cancers (Basel)* 12: 1663, 2020.
29. Ceballos MP, Rigalli JP, Cere LI, Semeniuk M, Catania VA and Ruiz ML: ABC transporters: Regulation and association with multidrug resistance in hepatocellular carcinoma and colorectal carcinoma. *Curr Med Chem* 26: 1224-1250, 2019.
30. Nagaraju GP, Farran B, Luong T and El-Rayes BF: Understanding the molecular mechanisms that regulate pancreatic cancer stem cell formation, stemness and chemoresistance: A brief overview. *Semin Cancer Biol* 88: 67-80, 2023.
31. He S and Tang S: WNT/ β -catenin signaling in the development of liver cancers. *Biomed Pharmacother* 132: 110851, 2020.
32. Schaefer KN, Bonello TT, Zhang S, Williams CE, Roberts DM, McKay DJ and Peifer M: Supramolecular assembly of the beta-catenin destruction complex and the effect of Wnt signaling on its localization, molecular size, and activity *in vivo*. *PLoS Genet* 14: e1007339, 2018.
33. Pfister AS and Kühl M: Of Wnts and ribosomes. *Prog Mol Biol Transl Sci* 153: 131-155, 2018.
34. Ma Y, Ma M, Sun J, Li W, Li Y, Guo X and Zhang H: CHIR-99021 regulates mitochondrial remodelling via β -catenin signalling and miRNA expression during endodermal differentiation. *J Cell Sci* 132: jcs229948, 2019.
35. Feng Z, Mabrouk I, Msuthwana P, Zhou Y, Song Y, Gong H, Li S, Min C, Ju A, Duan A, *et al*: In ovo injection of CHIR-99021 promotes feather follicles development via activating Wnt/ β -catenin signaling pathway during chick embryonic period. *Poult Sci* 101: 101825, 2022.
36. Delepine C, Pham VA, Tsang HWS and Sur M: GSK3 β inhibitor CHIR 99021 modulates cerebral organoid development through dose-dependent regulation of apoptosis, proliferation, differentiation and migration. *PLoS One* 16: e0251173, 2021.
37. Xu C, Xu Z, Zhang Y, Evert M, Calvisi DF and Chen X: β -Catenin signaling in hepatocellular carcinoma. *J Clin Invest* 132: e154515, 2022.
38. Leung RWH and Lee TKW: Wnt/ β -Catenin signaling as a driver of stemness and metabolic reprogramming in hepatocellular carcinoma. *Cancers (Basel)* 14: 5468, 2022.



Copyright © 2023 Wang and Zhu. This work is licensed under a Creative Commons Attribution-NonCommercial-NoDerivatives 4.0 International (CC BY-NC-ND 4.0) License.